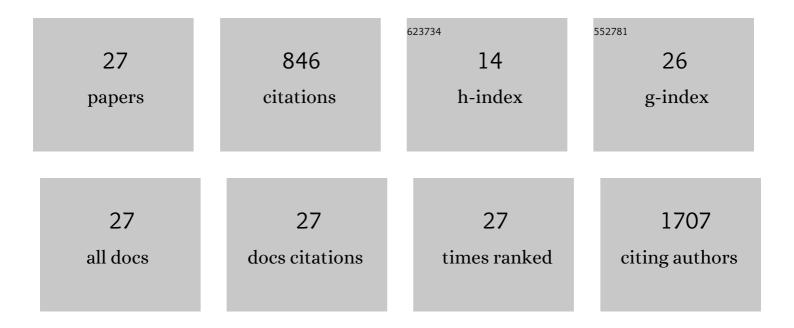
Yingchao Liu

List of Publications by Year in descending order

Source: https://exaly.com/author-pdf/5581181/publications.pdf Version: 2024-02-01



#	Article	IF	CITATIONS
1	Multimodality MRI-based radiomics approach to predict the posttreatment response of lung cancer brain metastases to gamma knife radiosurgery. European Radiology, 2022, 32, 2266-2276.	4.5	20
2	Consideration of transmembrane water exchange in pharmacokinetic model significantly improves the accuracy of DCE-MRI in estimating cellular density: A pilot study in glioblastoma multiforme. Magnetic Resonance Letters, 2022, 2, 243-254.	1.3	0
3	A water-soluble fluorescent probe for real-time visualization of Î ³ -glutamyl transpeptidase activity in living cells. Bioorganic and Medicinal Chemistry Letters, 2022, 68, 128762.	2.2	6
4	Convolutional neural network for accelerating the computation of the extended Tofts model in <scp>dynamic contrastâ€enhanced magnetic resonance imaging</scp> . Journal of Magnetic Resonance Imaging, 2021, 53, 1898-1910.	3.4	17
5	Deep learning–based detection and segmentation-assisted management of brain metastases. Neuro-Oncology, 2020, 22, 505-514.	1.2	69
6	Nâ€acetylglucosaminyltransferase I promotes glioma cell proliferation and migration through increasing the stability of the glucose transporter GLUT1. FEBS Letters, 2020, 594, 358-366.	2.8	12
7	Bazedoxifene enhances paclitaxel efficacy to suppress glioblastoma via altering Hippo/YAP pathway. Journal of Cancer, 2020, 11, 657-667.	2.5	8
8	Hypergraph membrane system based <mml:math <br="" xmlns:mml="http://www.w3.org/1998/Math/MathML">display="inline" id="d1e2639" altimg="si23.svg"> <mml:msup> <mml:mrow> <mml:mi>F </mml:mi> </mml:mrow> <mml:mrow> <mml:mn>2 fully convolutional neural network for brain tumor segmentation. Applied Soft Computing Journal, 2020, 94, 106454.</mml:mn></mml:mrow></mml:msup></mml:math>	1ml:n a12 > <td>າmໄນຜາດw></td>	າm ໄນ ຜາດw>
9	Shutter‧peed DCEâ€MRI Analyses of Human Glioblastoma Multiforme (GBM) Data. Journal of Magnetic Resonance Imaging, 2020, 52, 850-863.	3.4	18
10	A segmentation-independent volume rendering visualisation method might reduce redundant explorations and post-surgical complications of microvascular decompression. European Radiology, 2020, 30, 3823-3833.	4.5	3
11	Enhanced Î ³ -Glutamyltranspeptidase Imaging That Unravels the Glioma Recurrence in Post-radio/Chemotherapy Mixtures for Precise Pathology via Enzyme-Triggered Fluorescent Probe. Frontiers in Neuroscience, 2019, 13, 557.	2.8	9
12	Machine Learning Models for Multiparametric Glioma Grading With Quantitative Result Interpretations. Frontiers in Neuroscience, 2019, 12, 1046.	2.8	46
13	A Universal Intensity Standardization Method Based on a Many-to-One Weak-Paired Cycle Generative Adversarial Network for Magnetic Resonance Images. IEEE Transactions on Medical Imaging, 2019, 38, 2059-2069.	8.9	37
14	Quantitative dynamic susceptibility contrast perfusion-weighted imaging-guided customized gamma knife re-irradiation of recurrent high-grade gliomas. Journal of Neuro-Oncology, 2018, 139, 185-193.	2.9	8
15	Visualizing glioma margins by real-time tracking of Î ³ -glutamyltranspeptidase activity. Biomaterials, 2018, 173, 1-10.	11.4	50
16	Absolute CBV for the differentiation of recurrence and radionecrosis of brain metastases after gamma knife radiotherapy: a comparison with relative CBV. Clinical Radiology, 2018, 73, 758.e1-758.e7.	1.1	11
17	Postcontrast T1 Mapping for Differential Diagnosis of Recurrence and Radionecrosis after Gamma Knife Radiosurgery for Brain Metastasis. American Journal of Neuroradiology, 2018, 39, 1025-1031.	2.4	22
18	Association of ACVRL1 Genetic Polymorphisms with Arteriovenous Malformations: A Case-Control Study and Meta-Analysis. World Neurosurgery, 2017, 108, 690-697.	1.3	4

Yingchao Liu

#	Article	IF	CITATIONS
19	Juglone potentiates TRAIL-induced apoptosis in human melanoma cells via activating the ROS-p38-p53 pathway. Molecular Medicine Reports, 2017, 16, 9645-9651.	2.4	20
20	Rapid Capture and Analysis of Airborne Staphylococcus aureus in the Hospital Using a Microfluidic Chip. Micromachines, 2016, 7, 169.	2.9	23
21	A fluorescent turn-on probe for visualizing lysosomes in hypoxic tumor cells. Analyst, The, 2016, 141, 2879-2882.	3.5	31
22	Miro1 deficiency in amyotrophic lateral sclerosis. Frontiers in Aging Neuroscience, 2015, 7, 100.	3.4	55
23	lcariin inhibits TNF-α/IFN-γ induced inflammatory response via inhibition of the substance P and p38-MAPK signaling pathway in human keratinocytes. International Immunopharmacology, 2015, 29, 401-407.	3.8	82
24	Microfluidic chip for rapid analysis of cerebrospinal fluid infected with Staphylococcus aureus. Analytical Methods, 2014, 6, 2015-2019.	2.7	10
25	Activation of PI3K/Akt pathway by CD133-p85 interaction promotes tumorigenic capacity of glioma stem cells. Proceedings of the National Academy of Sciences of the United States of America, 2013, 110, 6829-6834.	7.1	232
26	Shotgun proteomic analysis of microdissected postmortem human pituitary using complementary two-dimensional liquid chromatography coupled with tandem mass spectrometer. Analytica Chimica Acta, 2011, 688, 183-190.	5.4	13
27	Proteomic analysis of prolactinoma cells by immuno-laser capture microdissection combined with online two-dimensional nano-scale liquid chromatography/mass spectrometry. Proteome Science, 2010, 8, 2.	1.7	24